Immunobiology 228 (2023) 152389

Contents lists available at ScienceDirect

Immunobiology

journal homepage: www.elsevier.com/locate/imbio

PD-L1 and PD-L2 immune checkpoint protein induction by type III interferon in non-small cell lung cancer cells

Trine Vilsbøll Larsen [a], Tina Fuglsang Daugaard [a], Hans Henrik Gad [b], Rune Hartmann [b], Anders Lade Nielsen [a,*]

[a] Department of Biomedicine, Aarhus University, Denmark
[b] Department of Molecular Biology and Genetics, Aarhus University, Denmark

ARTICLE INFO

Keywords:
Immunotherapy
Lung cancer
IFN signaling
IFNL

ABSTRACT

Introduction: Despite the clinical success of PD-1/PD-1-ligand immunotherapy in non-small cell lung cancer (NSCLC), the appearance of primary and acquired therapy resistance is a major challenge reflecting that the mechanisms regulating the expression of the PD-1-ligands PD-L1 and PD-L2 are not fully explored. Type I and II interferons (IFNs) induce PD-L1 and PD-L2 expression. Here, we examined if PD-L1 and PD-L2 expression also can be induced by type III IFN, IFN-λ, which is peculiarly important for airway epithelial surfaces.

Methods: In silico mRNA expression analysis of *PD-L1 (CD274)*, *PD-L2 (PDCD1LG2)*, and IFN- λ signaling signature genes in NSCLC tumors and cell lines was performed using RNA sequencing expression data from TCGA, OncoSG, and DepMap portals. IFN-λ-mediated induction of PD-L1 and PD-L2 expression in NSCLC cell lines was examined by real-time quantitative polymerase chain reaction and flow cytometry.

Results: IFNL genes encoding IFN- λ variants are expressed in the majority of NSCLC tumors and cell lines along with the *IFNLR1* and *IL10R2* genes encoding the IFN-λ receptor subunits. The expression of *PD-L1* and *PD-L2* mRNA is higher in NSCLC tumors with *IFNL* mRNA expression compared to tumors without *IFNL* expression. In the NSCLC cell line HCC827, stimulation with IFN-λ induced both an increase in *PD-L1* and *PD-L2* mRNA expression and cell surface abundance of the corresponding proteins. In the NSCLC cell line A427, displaying a low basal expression of *PD-L1* and *PD-L2* mRNA and corresponding proteins, stimulation with IFN-λ resulted in an induction of the former.

Conclusion: The type III IFN, IFN- λ, is capable of inducing PD-L1 and PD-L2 expression, at least in some NSCLC cells, and this regulation will need acknowledgment in the development of new diagnostic procedures, such as gene expression signature profiles, to improve PD-1/PD-1-ligand immunotherapy in NSCLC.

1. Introduction

Interferons (IFNs) possess antiviral and anti-cancer activity. The most recently discovered class of IFNs, type III IFN, consists of four homologous proteins, IFN-λ1, IFN-λ2, IFN-λ3, and IFN-λ4 (Kotenko et al., 2003; Prokunina-Olsson et al., 2013; Sheppard et al., 2003). All IFN-λ subtypes induce cellular responses through binding to their heterodimeric receptor consisting of subunits IL10R2 (IL10Rβ) and IFNλR1 (IL28Rα). The IL10R2 receptor subunit also participates in IL-10, IL-22, and IL-26 signaling (Walter, 2020). Whereas IL10R2 is ubiquitously expressed, IFNλR1 expression is more restricted and is preferentially expressed on cells present at barrier surfaces with high epithelial content such as the intestine, skin, and lung, and the current dogma is that IFN-λ protects the epithelium against viral infections (Sommereyns et al., 2008; Zanoni et al., 2017; Donnelly et al., 2004; Crotta et al., 2013). However, recent findings challenge this view since IFNλR1 is also expressed by a subset of immune cells (Zanoni et al., 2017). IFN-λ-signaling resembles that of type I IFN (IFN-α/β) (Zhou et al., 2007; Lasfar et al., 2019). Upon IFN-λ binding, the receptor-associated JAK1 and TYK1 kinases are activated, and this results in the formation of the ISGF3 transcription factor complex composed of STAT1, STAT2, and interferon response factor 9 (IRF9) (Wack et al., 2015). ISGF3 translocates to the nucleus where it binds interferon-sensitive response elements (ISRE) and regulates the expression of IFN-stimulated genes

* Corresponding author at: Department of Biomedicine, Faculty of Health, Aarhus University Skou Building 1115, 4N, Høegh-Guldbergsgade 10, DK-8000 Aarhus C, Denmark.
E-mail address: aln@biomed.au.dk (A.L. Nielsen).

https://doi.org/10.1016/j.imbio.2023.152389
Received 3 February 2023; Received in revised form 29 March 2023; Accepted 16 April 2023
Available online 18 April 2023

(ISGs), including the genes encoding the transcription factors IRF1 and IRF7 (Zhou et al., 2007; Lu et al., 2000). Besides, IFN-λ has also been shown to activate mitogen-activated protein (MAP) kinase pathways (Zhou et al., 2007; Brand et al., 2005). In the tumor microenvironment, both dendritic and cancer cells can produce type I and type III IFN (mainly IFN-λ1, but also IFN-λ2 and IFN-λ3) through activation of the TLR3 and cGAS-STING pathways in response to DNA released from dying or disrupted tumor cells (Chen et al., 2018; Vitiello et al., 2021; Deb et al., 2020; Hubert et al., 2020). IFN-λ is proposed to possess direct anti-tumor effects such as induction of tumor apoptosis and cell cycle arrest in several cancer types (Lasfar et al., 2019; Tezuka et al., 2012; Li et al., 2012; Fujie et al., 2011).

Antibody-based immunotherapy targeting the immune checkpoint PD-1/PD-1-ligand axis is a treatment option in cancer, including non-small cell lung cancer (NSCLC) (Sun et al., 2020). PD-L1 and PD-L2 are ligands for PD-1 and the interaction is normally involved in maintaining peripheral and central immune cell tolerance. When cancer cell membrane-located PD-1-ligands bind the PD-1 membrane receptor on anti-tumor T cells, the T cells can be inactivated, thus providing a way for cancer cells to escape tumor immunity (He et al., 2015). Anti-PD-1 and anti-PD-L1 antibodies can block this interaction, relieving PD-1-mediated immune suppression and regaining anti-tumor immunity (Iwai et al., 2002; Hirano et al., 2005). Despite the clinical success of PD-1/PD-L1 immunotherapy, therapy resistance, either primary or acquired, is a major challenge (Sun et al., 2020; Jenkins et al., 2018). In NSCLC, the response rate to PD-1/PD-L1 immunotherapy is only approximately 20% (Borghaei et al., 2015; Garon et al., 2015). During an anti-tumor immune response, cytokines and pro-inflammatory molecules are released into the tumor microenvironment where they can induce the expression of PD-1-ligands in cancer cells and other tumor microenvironment cells, leading to tumor immune escape, a phenomenon called adaptive immune resistance (Garcia-Diaz et al., 2019). IFN of type I and type II (IFN-γ) induces the expression of PD-1-ligands in cancer cells through the JAK-STAT signaling pathway, as well as through C-FOS (Garcia-Diaz et al., 2019; Morimoto et al., 2018; Shibahara et al., 2018; Lee et al., 2006). Garcia-Diaz et al. showed the existence of functional IRF1 binding sites in the *PD-L1* (*CD274*) and *PD-L2* (*PDCD1LG2*) promoters for activation by type II IFN and type I and II IFNs, respectively (Garcia-Diaz et al., 2019). Furthermore, a STAT1/STAT3 binding site in the *PD-L2* promoter was shown to have larger importance than the IRF1 binding site during activation by type I and II IFNs (Garcia-Diaz et al., 2019). The *PD-L1* promoter also contains two binding sites for IRF7 and upregulation of IRF7 expression independent of IFN-signaling increases *PD-L1* mRNA and PD-L1 protein expression in NSCLC cell lines (Lai et al., 2018).

To improve PD-1/PD-L1 cancer immunotherapy, it will be important to understand in depth the mechanisms that regulate PD-1-ligand expression. Because type III IFN resembles type I IFN in its downstream signaling pathway and is peculiarly important for airway epithelial surfaces, we here questioned whether type III IFN can upregulate PD-1-ligand expression in NSCLC cells.

2. Materials and methods

2.1. In silico mRNA expression analyses

2.1.1. cBioPortal analysis

The cBioPortal (https://www.cbioportal.org/) was used to access mRNA expression data of NSCLC patient tumors from The Cancer Genome Atlas (TCGA) project (Gao et al., 2013; Cerami et al., 2012). The TCGA Firehose Legacy studies NSCLC Lung Adenocarcinoma (LUAD, n = 586) and NSCLC Lung Squamous Cell Carcinoma (LUSC, n = 511) were used for analysis. Samples with no available expression data were removed before analysis. mRNA expression data for NSCLC patient adenocarcinoma tumors from the Singapore Oncology Data Portal (OncoSG) (n = 169) were used as a validation dataset (Chen et al., 2020). TCGA and OncoSG RNA sequencing (seq) data in the format V2 RNA-Seq by Expectation Maximization (RSEM) were log2-transformed using a pseudo-count of 1 before analysis.

2.1.2. DepMap portal analysis

The DepMap Portal (https://depmap.org/portal/interactive/) was used to access mRNA expression data of NSCLC cell lines (n = 163). Using a pseudo-count of 1, log2 transformed RNA seq transcript per million (TPM) gene expression data were used for analysis. For IFN-λ receptor co-expression analyses, the filter NSCLC was used to extract mRNA expression data from the Expression 21Q4 Public dataset. NSCLC cell lines with no available expression data were removed before analysis. For IFN signaling signature genes including *PD-L1* and *PD-L2*, the filter NSCLC adenocarcinoma was used to extract mRNA expression data from the Expression 22Q1 and 22Q2 Public dataset. NSCLC adenocarcinoma cell lines with no available expression data were removed before analysis and cell lines were sorted according to whether they had hotspot mutations in *EGFR* and *KRAS*.

2.2. Cell culture

Genetic characteristics, purchase, and growth of cell lines A549, H358, H1666, HCC827, H1650, PC9, H1993, H1568, H2228, H1975, H596, and A427 were as previously described (Larsen et al., 2023). One day before IFN stimulation, cells were seeded in triplicates in 6 well plates at a cell density resulting in 60–80% confluent cells at the time of harvest for RNA extraction or flow cytometry analysis. Cells were stimulated with 10 ng/mL IFN-γ (PeproTech, 300-02), 10 ng/mL IFN-λ1 (PeproTech, 300-02L), or 10 ng/mL IFN-λ3 (Dellgren et al., 2009) for 5 h, 24 h, 48 h or 72 h. Respective controls received an equal volume of PBS + 0.01% bovine serum albumin (Sigma-Aldrich, A2153), PBS, or PBS with 10% glycerol, as cells stimulated with IFN-γ, IFN-λ1, and IFN-λ3, respectively.

2.3. RNA extraction, cDNA synthesis, and RT-qPCR

RNA was extracted using Trizol (Sigma-Aldrich T90424). Thermo Scientific NanodropTM spectrophotometer was used to measure the purity and concentration of purified RNA. cDNA synthesis of 1 μg RNA was performed with iScript cDNA Synthesis Kit (Bio-Rad, 170-8890). RT-qPCR was carried out on a Roche LightCycler 480 platform with the following settings: heating 95 °C for 15 min, 40 cycles of PCR (95 °C for 30 sec, gene-specific annealing temperature for 30 sec, 72 °C for 30 sec), and final elongation at 72 °C for 1 min. Each reaction contained 1 μL cDNA (10 ng/μL), 0.125 μL forward primer (10 pmol/μL), 0.125 μL reverse primer (10 pmol/μL), 5 μL RealQ Plus 2× Master Mix Green (Ampliqon, A323402) and 3.750 μL Nuclease-free H2O. Genes with Ct-values ≥35 were considered not expressed. This is exemplified by *MX1* expression in IFN-unstimulated A427 control cells being below the limit of detection and accordingly imputed an RT-qPCR value corresponding to Ct = 35. Data analysis was done using the X_0 method (Thomsen et al., 2010) and *TBP* mRNA expression was used for normalization. *TBP* was stably expressed throughout experiments. Primer efficiencies were determined from a standard curve. The following primers and annealing temperatures were used; *TBP* forward 5′ AGGAGCCAAGAGTGAAGAACAG 3′ and reverse 5′ CCCAACTTCTGTACAACTCTAGC 3′ (60 °C). *PD-L1* forward 5′ ACTGTGAAAGTCAATGCCCCA 3′ and reverse 5′ GGTGACTGGATCCACAACCA 3′ (60 °C). *PD-L2* forward 5′ AGCCCTAAGAAAACAACTCTGTCA 3′ and reverse 5′ ACAGGTCTTTTTGTTGTG TCTTTTG 3′ (60 °C). *IRF1* forward 5′ CATGGCTGGGACATCAACAAG 3′ and reverse 5′ TGCTTTGTATCGGCCTGTGTG 3′ (60 °C). *IRF7* forward 5′ CCACGCTATACCATCTACCT 3′ and reverse 5′ TATCCAGGGAAGACACACC 3′ (60 °C). *IFNLR1* forward 5′ CAGCGTGTACCTGACATGGCTC 3′ and reverse 5′ CTTGGTTCCCGCACACTCTTCC 3′ (60 °C). *ISG56* forward 5′ CCTCCTTGGGTTCGTCTACA 3′ and reverse 5′ GGCTGATATCTGGGTGCCTA 3′ (58 °C). *MX1* forward 5′

ACCTACAGCTGGCTCCTGAA 3′ and reverse 5′ CGGCTAACGGATAAGCAGAG 3′ (58 °C). *OASL* forward 5′ AGGGTACAGATGGGACATCG 3′ and reverse 5′ AAGGGTTCACGATGAGGTTG 3′ (58 °C).

2.4. Flow cytometry

For flow cytometry, cells were detached using Accutase (Nordic Biosite, 423201), washed twice in stain buffer (PBS + 0.5% BSA + 0.09% sodium azide), and kept on ice. Cells were pre-incubated with 2.5 μL (2 mg/mL) human immunoglobulin (Ig) (CSL Behring, 108450) at 4 °C for 15 min. to block any unspecific antibody binding. Cells were stained in the total volume of 50 μL stain buffer solution containing 2.5 μL Ig from the blocking, 0.25 μL PD-L1 antibody (Brilliant Violet 421™ anti-human CD274 (B7-H1, PD-L1), BioLegend, 329713), 0.125 μL PD-L2 antibody (PE anti-human CD273 (B7-DC, PD-L2), BioLegend, 329605) and 0.5 μL LIVE/DEAD Fixable Near-IR (ThermoFisher Scientific, L34975) at 4 °C for 30 min. Cells were then washed three times in stain buffer and fixated in PBS containing 0.9% formaldehyde. One-Comp eBeads (ThermoFisher Scientific, 01–1111-41) stained with each antibody and ArC Amine Reactive Compensation Bead Kit (ThermoFisher Scientific, A10346) stained with LIVE/DEAD Fixable Near-IR were used for compensation. Fluorescence minus one (FMO) for each antibody was used for setting gates for positive cells. Cells were analyzed within 24 h using NovoCyte Quanteon 4025 (Agilent, Santa Clara, CA). Before experiments, all antibodies were titrated to determine staining concentration. Flow cytometry data were analyzed using FlowJo version 10 (BD Biosciences). The median fluorescence intensity (MFI) of stimulated cells was normalized to respective controls before statistical analysis.

2.5. Statistical analyses

Graphs and statistical analyses were created using Graphpad Prism version 9. Data are presented as mean and error bars as standard deviation except for box plots presented as median with percentiles. Significance was analyzed using unpaired *t*-test with correction for multiple comparisons using the Holm-Šidák method, Mann-Whitney test, one-way ANOVA followed by Šidák multiple comparison test, and two-way

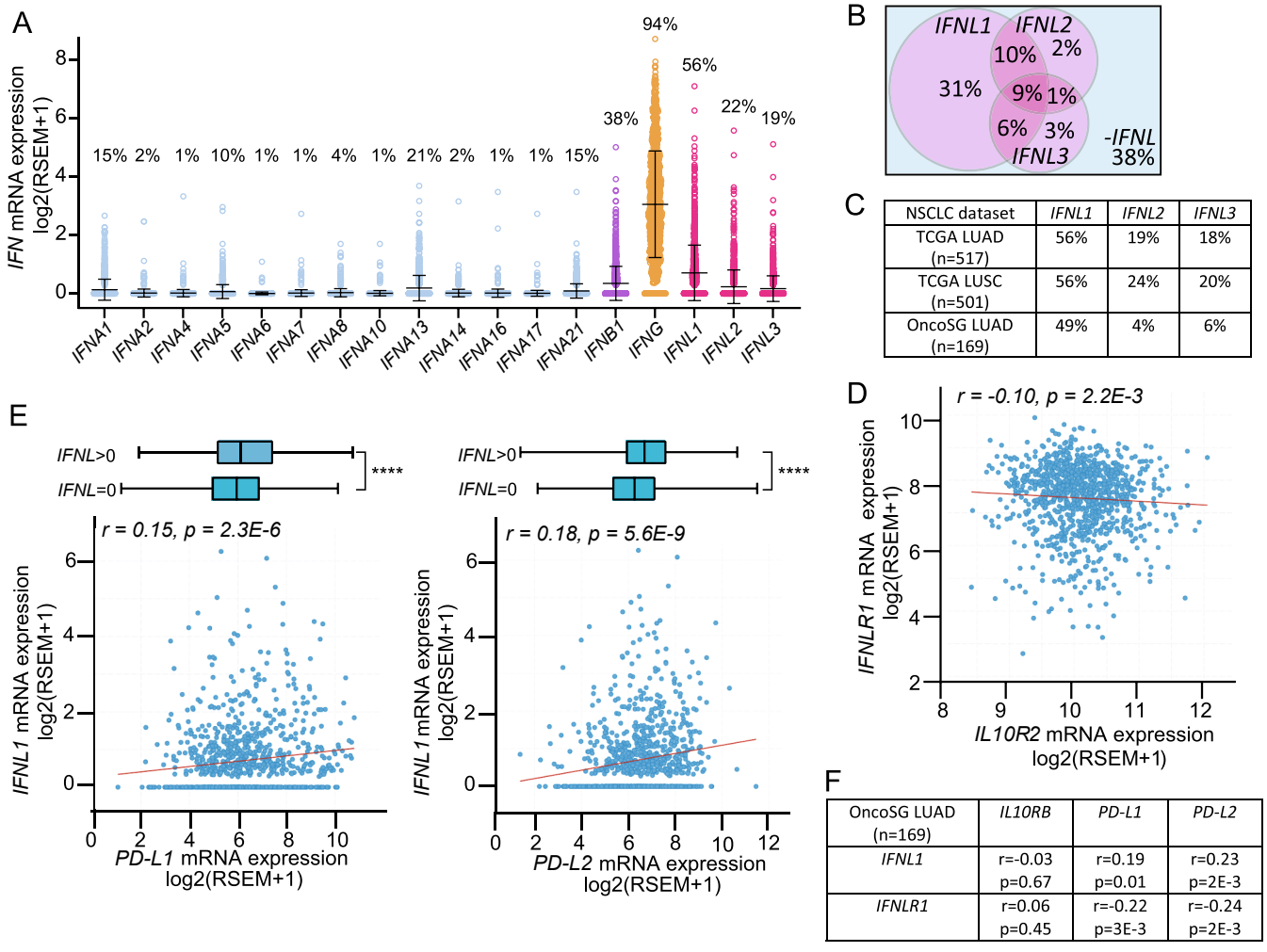

Fig. 1. *In silico* mRNA expression analyses of NSCLC tumors. (a) Analysis of 1018 NSCLC tumors (LUAD and LUSC) from TCGA Firehose Legacy studies available at cBioPortal for mRNA expression of *IFN* genes. Percentages of tumors with expression log2(RSEM + 1) > 0 of given *IFN* genes. (b) Venn diagram for the percentage of TCGA NSCLC tumors (LUAD and LUSC) expressing mRNA for *IFNL1*, *IFNL2,* and *IFNL3*. (c) Analyses of *IFNL* gene expression in TCGA LUAD, TCGA LUSC, and OncoSG LUAD. Percentages of tumors with *IFNL* mRNA expression, log2(RSEM + 1) > 0, are shown. (d) mRNA co-expression of *IFNLR1* and *IL10R2* mRNA in TCGA NSCLC dataset (LUAD and LUSC). Spearman correlation coefficient and corresponding p-value are shown. (e) mRNA co-expression of *IFNL1* and *PD-L1* (left panel) and *IFNL1* and *PD-L2* (right panel). Spearman correlation coefficients and corresponding p-values are shown. Upper boxplots are illustrating the difference in *PD-L1* and *PD-L2* mRNA expression between the population with *IFNL* mRNA expression log2(RSEM + 1) > 0, and the population without *IFNL* mRNA expression. Box represents the 25th percentile, median and 75th percentile. Whiskers represent minimum and maximum values. Mann-Whitney test is used to test for significance. **** p < 0.0001. (f) Spearman correlation analysis of mRNA expression in the validation dataset OncoSG LUAD (n = 169). Spearman correlation coefficients and corresponding p-values are shown.

ANOVA with interaction followed by Tukey's multiple comparisons tests as specified. Data were considered significant when p-value/adjusted p-value < 0.05.

3. Results

3.1. IFNL and its receptor co-express with PD-L1 in NSCLC cell lines and tumors

First, we examined if IFN-λ expression is present in NSCLC tumors. Merged mRNA expression data from TCGA LUAD and LUSC tumors (the TCGA NSCLC dataset) were used as a discovery dataset to examine if IFN-λ expression is present in individual tumors. Expression was assigned if log2(RSEM + 1) > 0. This showed that 62% of the tumors expressed at least one of the IFN-λ encoding genes *IFNL1, IFNL2,* and *IFNL3* (Fig. 1a and 1b). *IFNL1* is expressed in 56%, *IFNL2* in 22% and *IFNL3* in 19% of the NSCLC tumors (Fig. 1a). Moreover, in the TCGA NSCLC dataset expression of *IFNL1, IFNL2,* and *IFNL3* mRNA correlated (Table 1). The *IFNL* expression was similar in the individual TCGA LUSC and LUAD datasets (Fig. 1c). Examination of a validation dataset representing an independent cohort of lung adenocarcinoma tumor tissue samples, OncoSG (Chen et al., 2020), also revealed tumor expression of *IFNL1, IFNL2,* and *IFNL3* mRNA (Fig. 1c). With the vast majority of TCGA NSCLC tumors (94%) expressing *IFNG* mRNA, only a minority of tumors (3%) display *IFNL* mRNA expression without also having *IFNG* mRNA expression. More common is the existence of tumors with *IFNL* mRNA expression without also having *IFNB* mRNA expression (33%), *IFNA* mRNA expression (30%), or both *IFNB* and *IFNA* mRNA expression (19%). This supports the existence of a population of NSCLC tumors in which ISG transcriptional regulation can be concomitantly mediated by IFN-γ and IFN- λ, rather than concomitant between IFN- γ and IFN-α/β. Examining the mRNA expression of *IL10R2* and *IFNLR1* in the TCGA NSCLC dataset, showed co-expression in the tumors (Fig. 1d). However, the expression was not correlated in agreement with IL10R2 being a receptor for cytokines beyond IFN- λ (Fig. 1d). Thus, NSCLC tumors seem to possess the potential to support IFN-λ -mediated signaling.

The *PD-L1* and *PD-L2* genes can in cancer cells be activated by oncogenic driver mutations, various cytokines, and IFN-α/βand IFN-γ. In alignment with data showing that IFN- γ is an important activator of PD-1-ligand expression, we find that *PD-L1* and *PD-L2* mRNA expression is correlated with *IFNG* mRNA expression (Table 1) (Garcia-Diaz et al., 2019; Larsen et al., 2019). Induction of *PD-L1* and *PD-L2* expression in response to IFN- λ stimulation could also contribute to NSCLC tumor immune escape. mRNA expression analyses of TCGA and NSCLC tumors revealed neither correlation between *IFNL1* and *PD-L1* nor between *IFNL1* and *PD-L2* mRNA (Fig. 1e and 1f). Similar, neither *IFNL2* nor *IFNL3* mRNA displayed expression correlation in TCGA NSCLC tumors with *PD-L1* and *PD-L2* mRNA (Table 1). However, the expression of *PD-L1* and *PD-L2* mRNA was significantly higher in the population of tumors in the TCGA NSCLC dataset with *IFNL* mRNA expression (Fig. 1e, upper panels). ISG56 (*IFIT1)*, *MX1*, and *OASL* genes are well characterized to be IFN-λ response genes (Zhou et al., 2007; Doyle et al., 2006; Lauber et al., 2015), and the expression of these correlated with *IFNL* mRNA expression (Table 1). For *IRF1* and *IRF7* mRNA there were tendencies of correlation with *IFNL* mRNA expression (Table 1). Together this indicates that IFN-λ–signaling, across the NSCLC tumors, is not the major driver of *PD-L1* and *PD-L2* mRNA expression, but that IFN-λ-signaling could contribute in parallel with oncogenic drivers, cytokines, and IFNs of type I and type II, to confer the *PD-L1* and *PD-L2* mRNA expression levels present in the individual tumors.

The cellular heterogeneity and the associated complex regulation of *PD-L1* and *PD-L2* expression in NSCLC tumors could mask a contribution from IFN-λ signaling. To address this, we examined expression data for CCLE NSCLC cell lines. We observed co-expression of *IL10R2* and *IFNLR1* mRNA in most of the NSCLC cell lines (Fig. 2a). This supports that some NSCLC cell lines have the potential to support IFN-λ signaling. As also observed in NSCLC tumors, the expression of *IL10R2* and *IFNLR1* mRNA was not correlated (Fig. 2a). mRNA expression (log2(TPM + 1) > 0) of at least one of the IFN-λ genes *IFNL1, IFNL2,* and *IFNL3* was detected in the majority of the NSCLC lines (65%) but the expression levels were generally low (Fig. 2b and c). The expression of *IFNL1, IFNL2,* and *IFNL3* mRNA correlated (Table 1). Thus, the cancer cells in NSCLC tumors could represent one source of IFN- λ. We next examined the co-expression of *PD-L1* and *PD-L2* mRNA with *IFNL* mRNA. No significant expression correlations were observed (Fig. 2d and Table 1). Moreover, the expression of neither *PD-L1* nor *PD-L2* mRNA was significantly increased in the population of NSCLC cell lines possessing *IFNL* mRNA expression (Fig. 2d, upper panels). Notably, *IFNL* mRNA expression correlated with *ISG56*, *MX1*, and *OASL* mRNA expression, and there was a tendency of correlation with *IRF1* and *IRF7* mRNA expression (Table 1). This points out that across the NSCLC cell lines, the given level of intrinsic IFN-λ-signaling is not a major driver of *PD-L1* and

Table 1
Spearman correlation analysis in NSCLC mRNA expression datasets.

	TCGA NSCLC												
gene	*IFNL1*	*IFNL2*	*IFNL3*	*IFNLR1*	*IL10R2*	*IFNG*	*PD-L1*	*PD-L2*	*IRF1*	*IRF7*	*OASL*	*ISG56*	*MX1*
IFNL1		0.45 9E-52	0.36 2E-32	-0.08 0.01	0.12 2E-4	0.22 6E-12	0.15 2E-6	0.18 6E-9	0.27 1E-17	0.34 1E-28	0.54 6E-75	0.45 2E-51	0.44 2E-49
IFNL2	0.54 4E-11		0.43 3E-45	-0.06 0.07	0.08 1E-2	0.13 3E-5	0.13 6E-5	0.09 5E-3	0.16 6E-7	0.27 8E-10	0.40 4E-39	0.39 3E-38	0.42 9E-43
IFNL3	0.52 3E-10	0.59 1E-13		-0.03 0.33	0.08 0.01	0.12 8E-5	0.08 8E-3	0.09 6E-3	0.12 1E-4	0.21 5E-11	0.30 2E-22	0.33 2E-26	0.30 1E-21
IFNLR1	0.24 7E-3	0.12 0.17	0.21 0.02		-0.10 2E-3	-0.25 4E-16	-0.08 0.01	-0.15 2E-6	-0.27 1E-17	-0.19 2E-9	-0.15 2E-6	-0.00 0.92	0.07 0.02
IL10R2	-0.13 0.16	0.09 0.32	-0.04 0.66	0.03 0.73		0.10 1E-3	0.15 2E-6	0.29 3E-20	0.22 1E-12	0.26 2E-16	0.28 1E-19	0.34 4E-29	0.33 4E-27
IFNG	0.10 0.28	0.03 0.71	-0.01 0.89	0.04 0.62	0.03 0.77		0.46 2E-52	0.58 7E-90	0.77 6E-194	0.17 8E-8	0.39 4E-38	0.19 4E-9	0.23 7E-14
PD-L1	0.21 0.02	0.14 0.11	0.24 7E-3	0.18 0.05	-0.10 0.25	-0.15 0.09		0.74 4E-176	0.47 5E-55	0.02 0.50	0.27 1E-17	0.22 7E-13	0.28 3E-19
PD-L2	0.09 0.30	0.11 0.23	0.08 0.36	-0.09 0.30	-0.07 0.45	-0.19 0.03	0.76 9E-26		0.59 2E-95	0.07 0.02	0.39 5E-38	0.31 2E-23	0.27 4E-18
IRF1	0.28 1E-3	0.31 4E-4	0.32 2E-4	0.02 0.78	0.13 0.15	-0.05 0.58	0.33 2E-4	0.41 2E-6		0.32 2E-25	0.51 2E-67	0.29 1E-20	0.36 4E-31
IRF7	0.23 9E-3	0.32 2E-4	0.35 4E-5	0.16 0.07	0.13 0.16	-0.12 0.16	0.32 2E-4	0.16 0.07	0.35 5E-5		0.41 1E-40	0.51 1E-65	0.51 2E-65
OASL	0.50 1E-9	0.43 5E-7	0.34 1E-4	0.13 0.14	0.00 0.96	0.03 0.78	0.26 4E-3	0.27 2E-3	0.44 2E-7	0.36 3E-5		0.70 3E-148	0.64 7E-118
ISG56	0.47 3E-8	0.41 2E-6	0.37 2E-5	0.05 0.60	0.01 0.89	-0.03 0.76	0.37 2E-5	0.39 4E-6	0.49 5E-9	0.37 1E-5	0.78 1E-27		0.81 1E-228
MX1	0.43 4E-7	0.42 1E-6	0.45 1E-7	0.31 3E-4	0.17 0.06	0.03 0.74	0.36 4E-5	0.29 8E-4	0.51 1E-9	0.45 7E-8	0.59 2E-13	0.59 3E-13	
gene	*IFNL1*	*IFNL2*	*IFNL3*	*IFNLR1*	*IL10R2*	*IFNG*	*PD-L1*	*PD-L2*	*IRF1*	*IRF7*	*OASL*	*ISG56*	*MX1*
	CCLE NSCLC												

Spearman correlation coefficients (upper lines) with corresponding p-values (lower lines) for mRNA expression in NSCLC datasets. In green colour is shown correlation coefficients for the TCGA NSCLC dataset (the merged LUAD and LUSC datasets). In blue colour is shown correlation coefficients for the CCLE NSCLC dataset. Synonymous gene names: *IL10R2/IL10RB*; *PD-L1/CD274*; *PD-L2/PDCD1LG2*; *ISG56/IFIT1*.

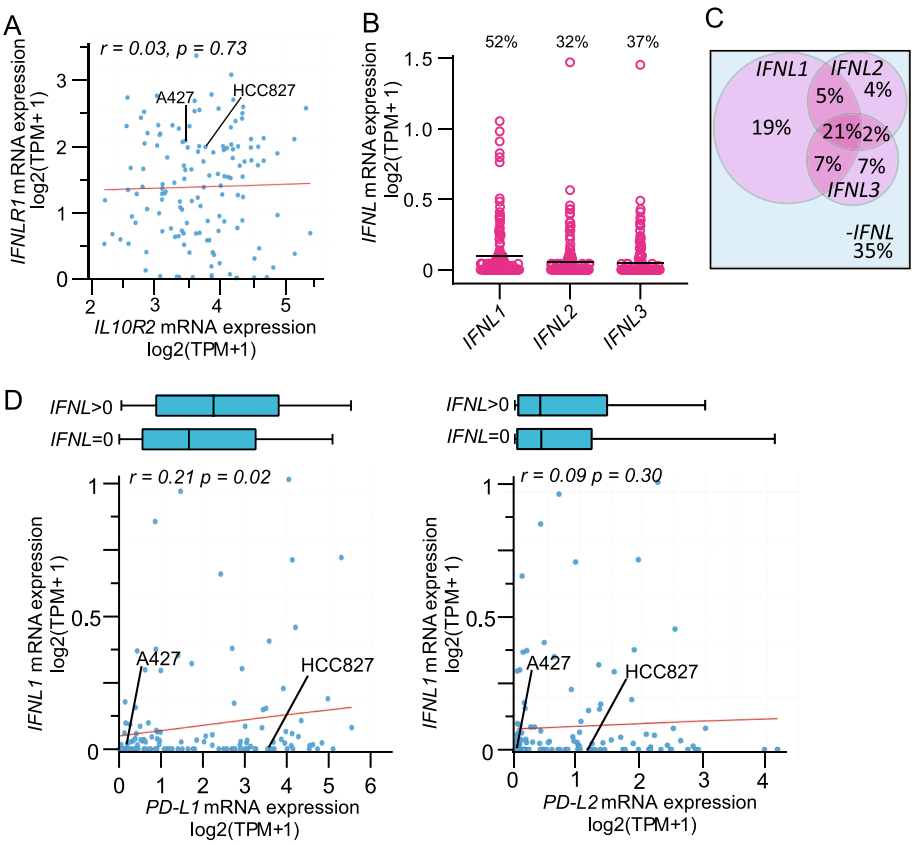

Fig. 2. *In silico* mRNA expression analyses of NSCLC cell lines. (a–d) Analysis of NSCLC cell lines from DepMap Portal Expression 21Q4 and 22Q2 Public dataset. (a) mRNA co-expression of *IFNLR1* and *IL10R2*. Spearman correlation coefficient and corresponding p-value are shown. (b) mRNA expression of *IFNL* genes (horizontal line represents mean). Percentages of cell lines with *IFNL* mRNA expression log2 (RSEM + 1) > 0 are shown. (c) Venn diagram for the percentage of NSCLC cell lines expressing mRNA for *IFNL1*, *IFNL2*, and *IFNL3*. (d) mRNA co-expression of *IFNL1* with *PD-L1* and *PD-L2*. Cell lines HCC827 and A427 are annotated. Spearman correlation coefficient and corresponding p-value are shown. Upper boxplots are illustrating the difference in *PD-L1* and *PD-L2* expression between the population with intrinsic *IFNL* expression, log2(TPM + 1) > 0, and the population without intrinsic *IFNL* expression. Box represents the 25th percentile, median and 75th percentile. Whiskers represent minimum and maximum values. Mann-Whitney test is used to test for significance.

PD-L2 mRNA expression. But the data also indicate that NSCLC cell lines can have a gene-expression signature that could support signaling by IFN-λ following *in vitro* stimulation.

3.2. IFN- λ induce PD-L1 and PD-L2 mRNA expression in HCC827 cells

The NSCLC cell line HCC827 harbors an oncogenic mutation in an amplified epidermal growth factor receptor (*EGFR)* gene with resulting ligand-independent activation of EGFR. HCC827 cells express PD-L1 and PD-L2 and the expression of both PD-1-ligands is stimulated by IFN-γ (Garcia-Diaz et al., 2019; Shibahara et al., 2018; Gao et al., 2018). Moreover, regulation of PD-L1 by type I IFN in HCC827 cells was suggested given that IFN αR1 depletion abrogated PD-L1 expression (Gong et al., 2020). We note that HCC827 cells express *IL10R2* and *IFNLR1* mRNA (Fig. 2a). Stimulating HCC827 cells with the representative type III IFN, IFN-λ3, did not result in altered *IFNLR1* mRNA expression

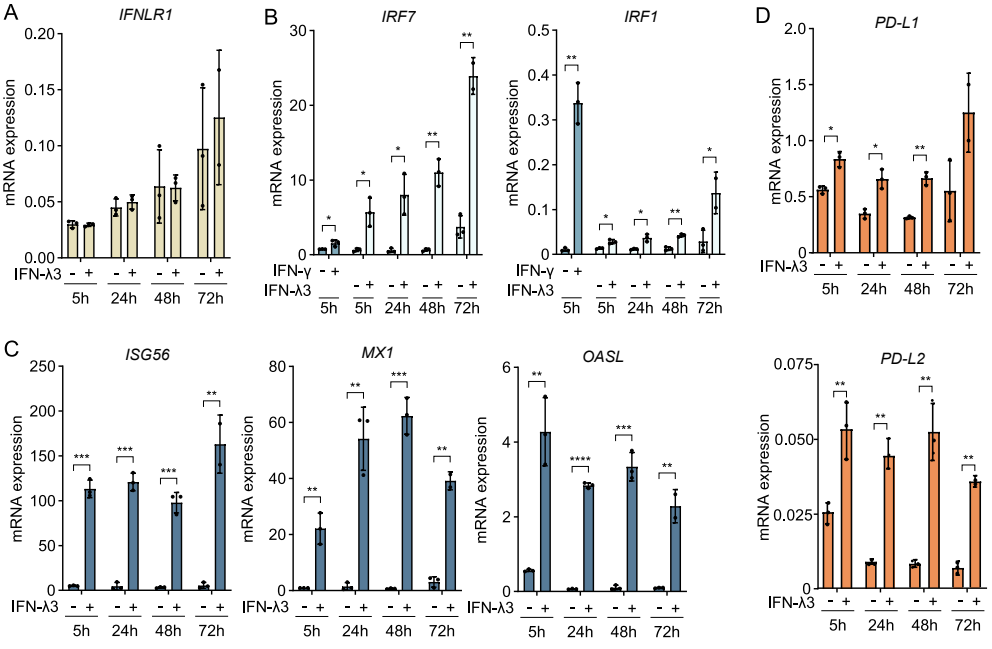

Fig. 3. IFN-λ3 induces *PD-L1* and *PD-L2* mRNA expression in HCC827 cells. (a–d) Cells were stimulated with 10 ng/mL IFN-λ3. In panel b cells were stimulated with 10 ng/mL IFN-γ. N = 3 for all time points and treatments except for IFN-λ3 at 72 h where N = 2. Stimulation is examined against respective untreated controls at each time point using multiple unpaired t-tests with correction for multiple comparisons using the Holm-Šidák method. * $p < 0.05$; ** $p < 0.01$; *** $p < 0.001$; **** $p < 0.0001$. mRNA expression is given relative to *TBP*.

supporting lack of autoregulation between IFN-λ and the cognate receptor (Fig. 3a). The IFN-λ signaling cascade is characterized by the induced expression of primarily IRF7 of the IRFs, which subsequently confers additional ISG induction (Zhou et al., 2007). In HCC827 cells, stimulation with IFN-λ induced the expression of *IRF7* mRNA at all the time endpoints (Fig. 3b). The IFN-λ signaling cascade was shown to also induce *IRF1* expression, but with IFN-γ signaling being a more pronounced *IRF1* inducer (Platanias, 2005; Der et al., 1998). In alignment, stimulation with IFN-λ in HCC827 cells resulted in less induction of *IRF1* mRNA relative to *IRF7* mRNA expression, whereas stimulation with IFN-γ, at least at the single time point examined (5 h), the *vice versa* was observed (Fig. 3b). *ISG56*, *MX1*, and *OASL* are characterized to be IFN-λ inducible genes (Zhou et al., 2007), and their mRNA expression increased upon IFN-λ stimulation (Fig. 3c). Altogether, these results indicate that HCC827 cells are responsive toward IFN-λ–mediated signaling.

We next examined the mRNA expression of *PD-L1* mRNA after IFN-λ stimulation. At 5, 24, and 48 h of IFN-λ stimulation, *PD-L1* mRNA expression was significantly upregulated (Fig. 3d). We also examined if IFN-λ3 induces *PD-L2* mRNA expression. IFN-λ stimulation significantly upregulated *PD-L2* mRNA expression at all the time endpoints (Fig. 3d). Noteworthy, we observed more pronounced IFN-λ-mediated induction of *PD-L2* mRNA expression compared to *PD-L1* mRNA expression (mean fold change induction at different time points relative to respective

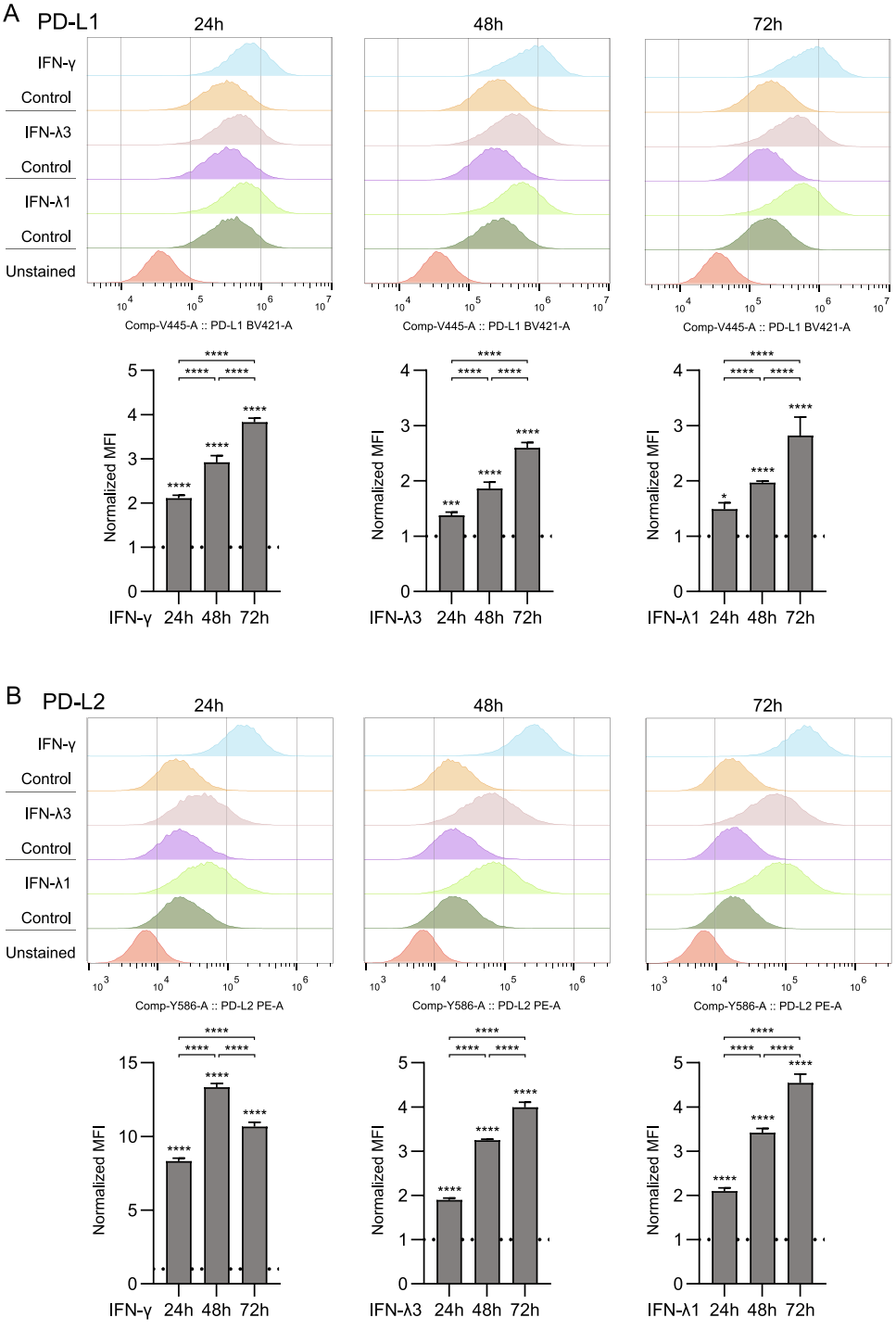

Fig. 4. IFN-λ and IFN-γ induce PD-L1 and PD-L2 cell surface protein expression in HCC827 cells. Flow cytometry analysis of a PD-L1 and b PD-L2 cell surface protein expression in HCC827 cells after stimulation with 10 ng/mL IFN-λ1, IFN-λ3, or IFN-γ for 24, 48 h, and 72 h compared to respective controls. Upper panels: Representative histogram of cell surface protein expression. Unstained represents FMO of a PD-L1 and b PD-L2. Lower panels: Cell surface protein expression of cells stimulated with IFN-γ (left), IFN-λ3 (middle), or IFN-λ1 (right) normalized to respective controls (controls represented by dotted line). N = 3 for all time points and treatments. Two-way ANOVA with interaction followed by Tukey's multiple comparisons tests. Adjusted p-value; * $p < 0.05$; ** $p < 0.01$; *** $p < 0.001$; **** $p < 0.0001$.

controls ranged from 1.48 to 2.11 for *PD-L1* and from 2.15 to 6.31 for *PD-L2*). We notice that the more pronounced *PD-L2* mRNA induction is in line with observations by Garcia-Diaz et al. showing a more profound induction of PD-L2 expression by IFN-β (Garcia-Diaz et al., 2019).

3.3. IFN-λ induces PD-1-ligand cell surface expression in HCC827 cells

To show if the IFN-λ-mediated increase in *PD-L1* and *PD-L2* mRNA expression in HCC827 cells translates to induced cell surface PD-L1 and PD-L2 protein expression, we performed flow cytometry analyses. We stimulated HCC827 cells with IFN-λ1 or IFN-λ3. In addition, we stimulated with IFN-γ as a positive control for induced PD-L1 and PD-L2 cell surface expression (Garcia-Diaz et al., 2019). IFN-λ1, IFN-λ3, and IFN-γ stimulation upregulated cell surface PD-L1 protein expression (Fig. 4a). The PD-L1 protein expression increased over time resulting in the highest PD-L1 expression at 72 h for both IFN-λ1, IFN-λ3, and IFN-γ stimulation (Fig. 4a). PD-L2 cell surface expression also increased upon IFN-λ1, IFN-λ3 and IFN-γ stimulations (Fig. 4b). Like for PD-L1, IFN-λ1 and IFN-λ3 stimulation resulted in highest PD-L2 expression at 72 h, whereas PD-L2 surface expression peaked at 48 h upon stimulation with IFN-γ (Fig. 4b). At all examined time points, IFN-λ1, IFN-λ3, and IFN-γ stimulations induced a more pronounced PD-L2 protein expression response relative to PD-L1 (Fig. 4a and b).

3.4. IFN-λ induces PD-L1 mRNA expression in A427 cells

We wanted to examine IFN-λ-mediated regulation of PD-L1 and PD-L2 in another NSCLC cell line. For this, we used the NSCLC cell line A427, which harbors an oncogenic mutation in the *KRAS* gene. A427 cells express *IL10R2* and *IFNLR1* mRNA and have a low *PD-L1* and *PD-L2* mRNA expression compared to HCC827 cells (Fig. 2a and d). As also observed in HCC827 cells, the expression of *IFNLR1* mRNA was not induced by IFN-λ3 in A427 cells (Fig. 5a). IFN-λ3 induced *IRF7* mRNA expression, and to a lesser extent *IRF1* mRNA expression (Fig. 5b). Moreover, IFN-λ3 induced the mRNA expression of *ISG56*, *MX1*, and *OASL* (Fig. 5c). Together this verifying that the IFN-λ signaling pathway could be activated in A427 cells.

IFN-λ3 stimulation mediated an increase in *PD-L1* mRNA expression (Fig. 5d). The induction of *PD-L1* mRNA expression in A427 cells was comparable to the induction in HCC827 cells. The *PD-L2* mRNA expression levels in both control and IFN-λ3 stimulated A427 cells were below the detection levels in RT-qPCR (all Ct-values ≥ 35). *PD-L2* mRNA expression below the limit of detection was also observed after IFN-γ stimulation (data not shown).

We next examined the PD-L1 and PD-L2 cell surface expression for A427 cells. A relatively low basic amount of PD-L1 and PD-L2 expression was observed (Fig. 6a and 6b). This is in alignment with the *PD-L1* and *PD-L2* mRNA expression levels in A427 cells. IFN-λ1 and IFN-λ3 stimulation had a minimal increasing effect on the PD-L1 cell surface expression, whereas the increase was more pronounced with IFN-γ stimulation, and this in a time point-depending manner (Fig. 6a). IFN-λ1 and IFN-λ3 stimulation did not increased PD-L2 surface expression (Fig. 6b). Albeit formally statistical significant, the increase in PD-L2 cell surface expression by IFN-γ was negligible (Fig. 6b). Thus, despite the presence of a functional IFN-λ-signaling cascade in A427 cells is the IFN-λ–mediated stimulation of PD-L1 and PD-L2 cell surface expression impeded relative to HCC827 cells.

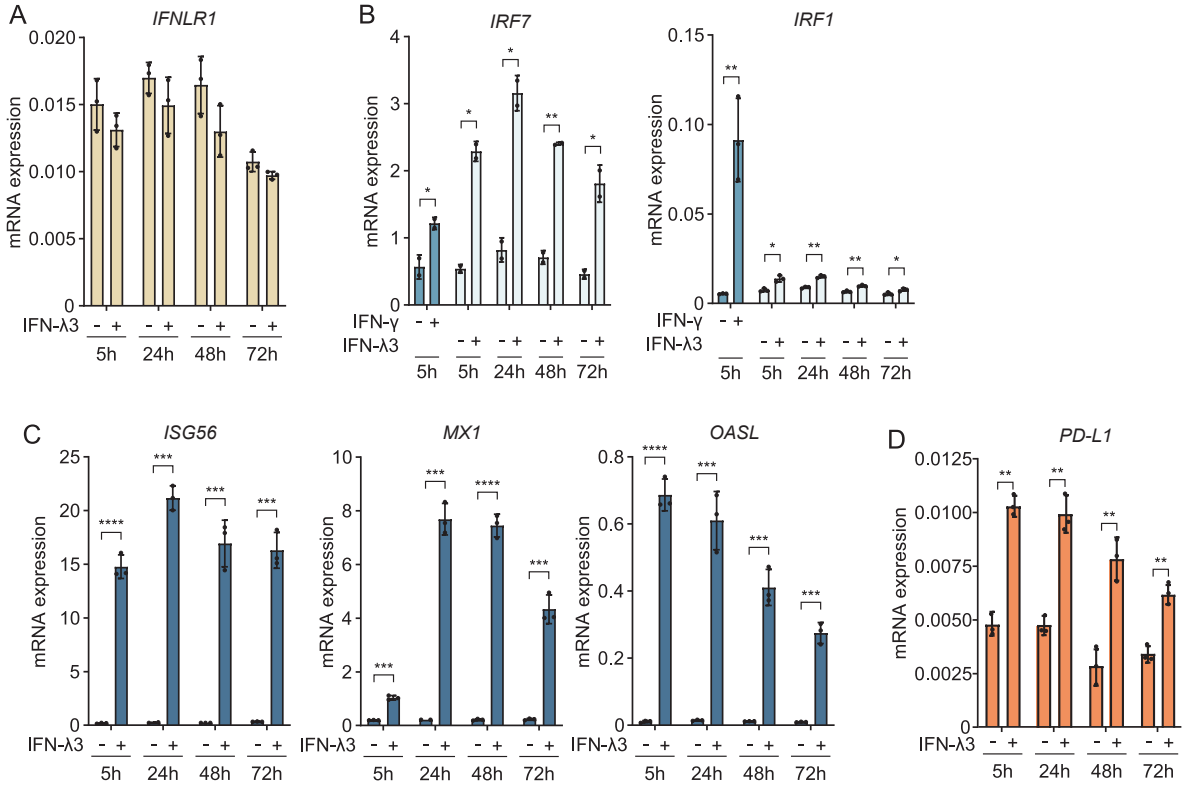

Fig. 5. IFN-λ3 induces *PD-L1* mRNA expression in A427 cells. (a–d) Cells stimulated with 10 ng/mL IFN-λ3. In panel b cells werestimulated with 10 ng/mL IFN-γ. N = 3 except for control at 24 h for *ISG56* and *MX1* where N = 2, and for *IRF7* where N = 2 for all time endpoints and treatments. Stimulation is examined against respective untreated controls at each time point using multiple unpaired t-tests with correction for multiple comparisons using the Holm-Šidák method. * $p < 0.05$; ** $p < 0.01$; *** $p < 0.001$; **** $p < 0.0001$. *MX1* expression in IFN-unstimulated cells was below the limit of detection and imputed an RT-qPCR value corresponding to Ct = 35. mRNA expression is given relative to *TBP*. In panel c was OASL protein induction analyzed by western blotting using H3 as a control for equal loading of sample material.

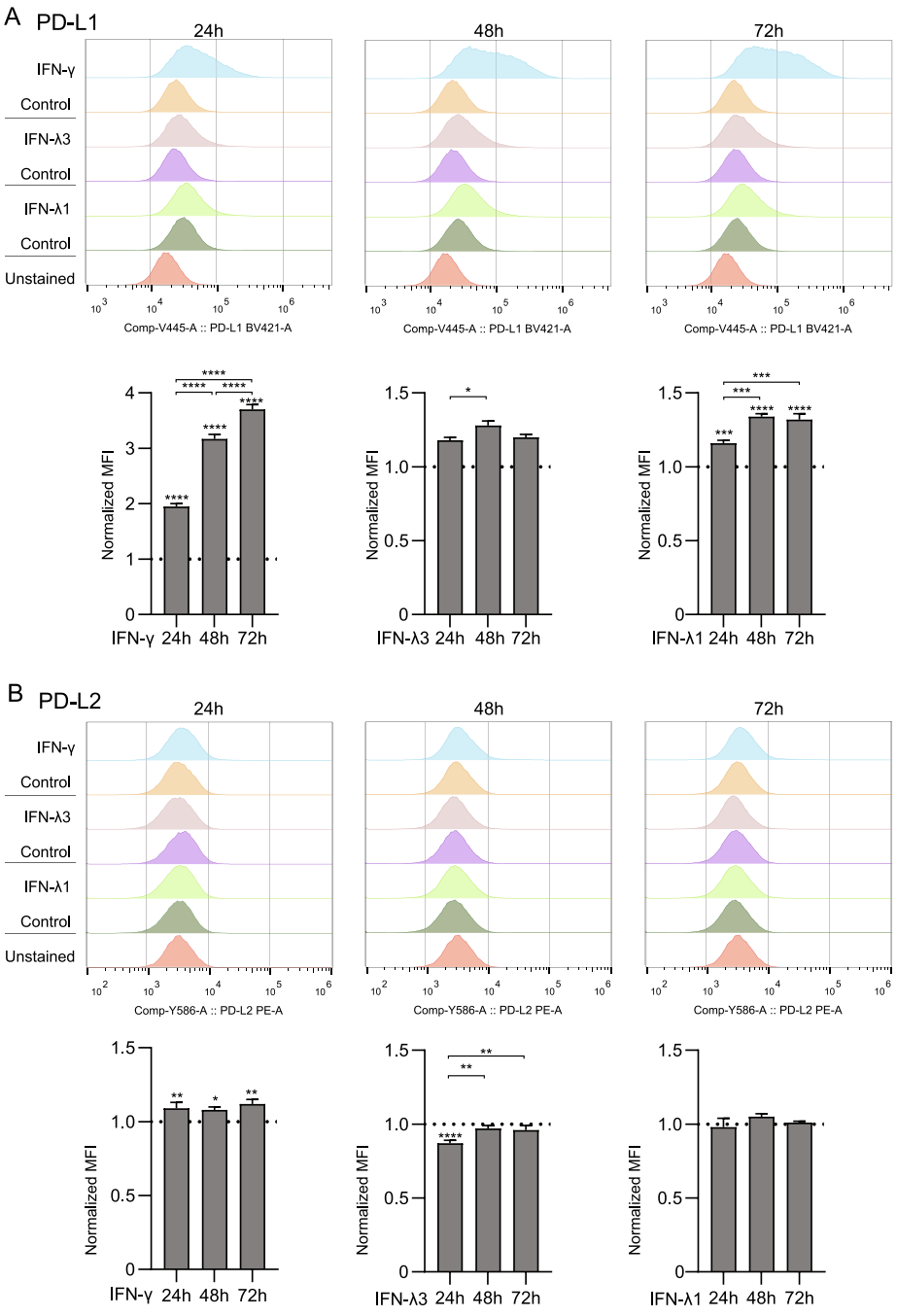

Fig. 6. IFN-λ modestly induces PD-L1 cell surface protein expression in A427 cells. Flow cytometry analysis of a PD-L1 and b PD-L2 cell surface protein expression in A427 cells after stimulation with 10 ng/mL IFN-λ1, IFN-λ3, or IFN-γ for 24 h, 48 h, and 72 h compared to respective controls. Upper panels: Representative histogram of cell surface protein expression. Unstained represents FMO of a PD-L1 and b PD-L2. Lower panels: Cell surface protein expression of cells stimulated with IFN-γ (left), IFN-λ3 (middle), or IFN-λ1 (right) normalized to respective controls (controls represented by dotted line). N = 3 for all time points and treatments except for control for IFN-γ at 72 h where N = 2. Statistics: Two-way ANOVA with interaction followed by Tukey's multiple comparisons tests. Adjusted p-value; * $p < 0.05$; ** $p < 0.01$; *** $p < 0.001$; **** $p < 0.0001$; ns, not significant.

3.5. PD-L1 and PD-L2 mRNA induction by IFN- λin various NSCLC cell line genetic backgrounds

Activating mutations in *EGFR* and *KRAS* were previously shown to confer transcriptional regulatory landscapes impacting *PD-L1* and *PD-L2* mRNA expression (Shibahara et al., 2018; Ayers et al., 2017; Sumimoto et al., 2016), as well as to differently sustain IFN-λ-mediated growth inhibitory and apoptotic effects (Tezuka et al., 2012; Li et al., 2012; Fujie et al., 2011). On top of this, increasing the expression of IRF7 can in an IFN-signaling independent mechanism stimulate the expression of PD-L1 (Lai et al., 2018). With the lower basal expression of *PD-L1* and *PD-L2* in A427 cells relative to HCC827 cells, we questioned if this was reflecting a difference in the expression of IRF7, as well as other IFN-signaling factors, between NSCLC cells with *EGFR* and *KRAS*-mutations. In extracted DepMap portal expression data from NSCLC adenocarcinoma cell lines with either *EGFR* or *KRAS* mutations, including HCC827 and A427 cells, no significant differences in the expression of IFN-signaling factors were observed (Fig. 7). Furthermore, no basal *PD-L1* and *PD-L2* mRNA expression differences were systematically observed by comparing cell lines with *EGFR* and *KRAS* mutations (Fig. 7). But we notice the presence of a considerable variation in *PD-L1* and *PD-L2* mRNA expression among the cell lines (Fig. 7). Finally, we examined *PD-L1* and *PD-L2* mRNA induction by IFN-λ in a series of NSCLC cell lines (Table 2). In A549 cells, which like A427 cells harbor a *KRAS* mutation, both *PD-L1* and *PD-L2* mRNA expression was increased (Table 2). In PC9 cells, which like HCC827 cells harbor an *EGFR* mutation, *PD-L1* induction was modest and *PD-L2* induction was 2-fold (Table 2). This further indicates that the *EGFR* and *KRAS* oncogenic driver backgrounds are not major determinants for defining *PD-L1* and *PD-L2* mRNA induction as a consequence of IFN- λ stimulation. Among

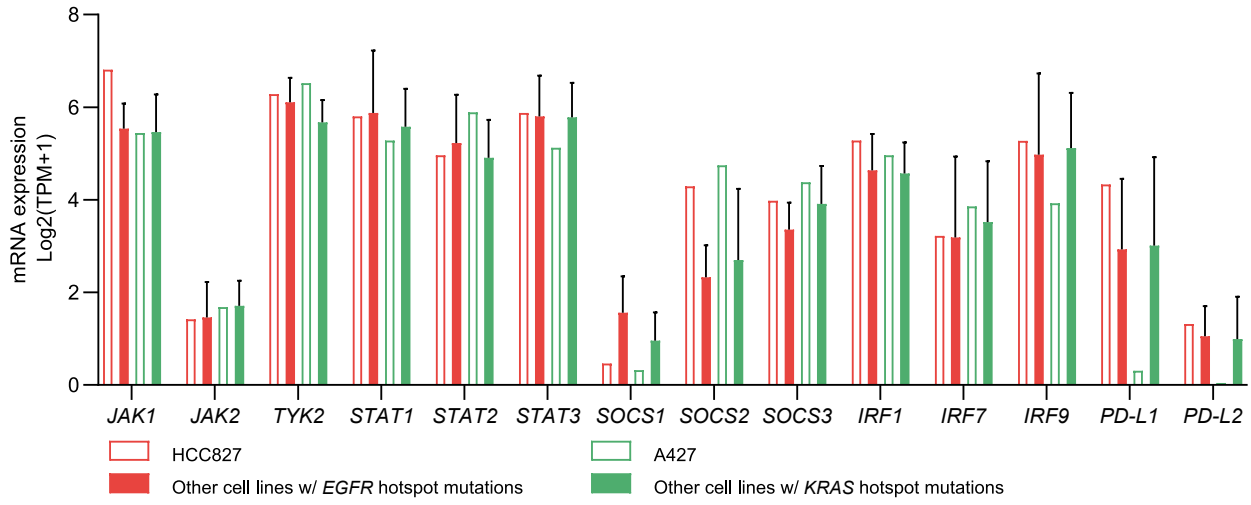

Fig. 7. IFN signature gene expression in NSCLC cell lines. mRNA expression analysis of IFN signaling signature genes, *PD-L1*, and *PD-L2* in HCC827, A427, and additional NSCLC cell lines with hotspot mutations in *EGFR* (N = 9) or *KRAS* (N = 26) using the DepMap Portal Expression 22Q1 and 22Q2 public datasets. One-way ANOVA followed by Šidák multiple comparison testing did not reveal significant differences.

Table 2
Mrna expression in ifn- λ stimulated NSCLC cell lines.

	PD-L1 mRNA		*PD-L2* mRNA		*ISG56* mRNA	
Cell line	Exp	FC + IFN- λ	Exp	FC + IFN- λ	Exp	FC + IFN- λ
HCC827	4.3	4.6	1.3	7.0	1.4	18.6
H358	3.8	1.3	0.3	1.8	2.8	13.0
H596	2.8	0.9	1.6	1.2	6.7	3.2
H1568	2.1	1.1	0.1	1.0	0.7	13.0
H1650	2.2	1.4	0.8	1.4	6.4	1.2
H1666	1.4	1.2	1.6	1.1	1.9	32.4
H1975	3.3	4.8	1.5	8.1	4.3	5.3
H1993	nd	1.3	nd	1.0	nd	3.6
H2228	3.4	1.5	2.3	1.7	2.6	18.2
A427	0.3	4.4	0.0	nd	0.7	62.1
A549	1.8	1.7	0.5	4.3	0.8	103.2
PC9	2.1	1.2	1.1	2.1	0.5	134.0

PD-L1, *PD-L2*, and *ISG56 (IFIT1)* mRNA expression normalized to mRNA expression of *TBP* and fold change (FC) in expression after 48 h stimulation with IFN- λ3. Exp, RNA sequencing determined expression levels without IFN- λ stimulation extracted from the DepMap portal in Log_2(transcripts per million (TPM) + 1). nd, expression data not available.

all the NSCLC cell lines, expression of *PD-L1* and *PD-L2* mRNA was increased to various degrees, but in general modest, following stimulation with IFN-λ (Table 2). A control gene for IFN-λ signaling, *ISG56*, displayed an increased mRNA expression in most cell lines and with the modest induction in H596 and H1650 cells assigned the high basal mRNA expression level in these particular cell lines (Table 2). For *PD-L1* and *PD-L2* there was no clear association between the basal level of mRNA expression and the degree of induction mediated by IFN- λ (Table 2). We conclude that across NSCLC cell lines, a large degree of heterogeneity is present concerning the impact of IFN- λ stimulation to mediate induced *PD-L1* and *PD-L2* mRNA expression.

4. Discussion

The hereby described observation that type III IFN, IFN- λ, has the potential to induce PD-L1 and PD-L2 expression has implications for PD-1/PD-1-ligand axis immunotherapy in NSCLC patients. The importance of detailed knowledge concerning PD-1-ligand regulation is dual with both its impact on improved diagnostics to identify immunotherapy responders and for developing immunotherapy based on the suppression of PD-1-ligand expression. The golden standard to identify NSCLC patients most likely responding to immunotherapy is to quantify the PD-L1 positive percentage of tumor cells by immunohistochemical analysis of a biopsy and subsequently offer immunotherapy to patients that display tumor PD-L1 expression positivity (Udall et al., 2018). A considerable fraction of the treated patients will not respond, and actual responders are present among the untreated patients (Borghaei et al., 2015; Garon et al., 2015; Malhotra et al., 2017; Fehrenbacher et al., 2016; Reck et al., 2016). Thus, diagnostic procedures, which go beyond direct immunological-based PD-L1 expression estimates are needed. For this is the use of tumor-based gene-expression signatures for oncogenic signaling and immune signaling controlling PD-L1 expression status appealing (Mehnert et al., 2017; Hwang et al., 2020). IFN signaling signatures are particularly promising due to the known stimulation of PD-L1 expression by type I and type II IFN (Garcia-Diaz et al., 2019; Morimoto et al., 2018; Ayers et al., 2017). That type III IFN, at least in some NSCLC cell lines, possesses the capability to induce PD-L1 expression highlights this signaling pathway also should be included in gene expression signatures used for immunotherapy diagnostics. We acknowledge that type I and type III IFN signaling pathways are largely overlapping, and, accordingly, many features of the IFN-λ signaling pathway are already included in existing gene expression signatures for IFN type I signaling. Nevertheless, the straightforward inclusion of *IFNL1*, *IFNL2,* and *IFNL3* mRNA expression data, similar to *IFNA*, *IFNB*, and *IFNG* mRNA expression data, could have immediate potential to improve diagnostic gene expression signatures. Three classes of NSCLC tumors were identified based on TCGA mRNA expression data: tumors without type I IFN gene expression but with type III IFN gene expression, tumors with type I IFN gene expression but without type III IFN gene expression, and tumors with both type I and type III IFN gene expression. On top of this, most NSCLC tumors possessed type II IFN gene expression. With *PD-L1* and *PD-L2* being ISGs, which in addition are activated by constitutive oncolytic pathways, the observation of also IFN-λ-mediated induction contributes to the mechanistic understanding of the time-spatial expression of PD-1-ligands in NSCLC tumors. Both inter- and intra-tumor heterogeneity of PD-1-ligand expression is widely documented (Haragan et al., 2019) and that type III IFN could be a contributor to this, beyond type I and type II IFNs, needs acknowledgment. We find it of importance that in NSCLC, IFN-λ anti-tumor effects were shown to be driver mutation-specific as IFN-λ mediates growth inhibitory and apoptotic effects in *EGFR*-mutated but not in *KRAS*-mutated NSCLC cells despite functional IFN-λ signaling pathways in both cell types (Tezuka et al., 2012; Li et al., 2012; Fujie et al., 2011). In this line, we also find that IFN-λ signaling is functional in both *KRAS*-mutated A427 and *EGFR*-mutated HCC827 cells since we observed IFN-λ

mediated induction of *ISG56*, *OASL*, *MX1*, *IRF1,* and *IRF7*. This further agrees with our results derived from mRNA expression data for HCC827, A427, and other NSCLC adenocarcinoma cell lines with either *EGFR* or *KRAS* mutations showing that the expression of IFN-λ signaling factors did not differ between the two genetic backgrounds. The basal mRNA and cell surface protein expression for PD-L1 and PD-L2 was lower in A427 cells compared to HCC827 cells. Whereas *PD-L1* and *PD-L2* mRNA expression increased upon IFN-λ stimulation in HCC827 cells, only an increase in *PD-L1* mRNA expression was detected in A427 cells. Notably, the fold-change in *PD-L1* mRNA expression following IFN-λ stimulation was similar in HCC827 and A427 cells. PD-L1 and PD-L2 cell surface abundance increased upon IFN-λ stimulation in HCC827 cells, but only a modest induction of PD-L1 was observed in A427 cells. Thus, the difference in induction of PD-1-ligand cell surface expression between HCC827 and A427 cells cannot be accounted specifically as a result of differences in promoter interacting *trans*-factors and IFN-signalling factors in the *KRAS*-mutated and *EGFR*-mutated cellular backgrounds. To this end, PD-L1 is also regulated on the post-transcriptional and post-translational levels. This is exemplified by the regulation of *PD-L1* mRNA stability by miRNAs; the regulation of PD-L1 protein translocation at the cancer cell membrane by CMTM4 and CMTM6; and the regulation of PD-L1 localization and stability from various post-translational modifications (Hu et al., 2021; Burr et al., 2017; Mezzadra et al., 2017; Skafi et al., 2020). We also note that an examination of OASL protein induction by IFN-γ and IFN- λ stimulation in HCC827 cells and A427 cells also revealed that induction at protein level was unproportioned to induction at mRNA level (data not shown). Further studies are required to determine the exact background for the variability in IFN- λ -mediated induction of PD-1-ligands in different NSCLC cell lines.

PD-L1-directed antibodies with resulting blocking effect for the interaction between PD-L1 and T-cell located PD-1 are used in immunotherapy to activate tumor T-cells (Sun et al., 2020; He et al., 2015; Iwai et al., 2002; Hirano et al., 2005; Jenkins et al., 2018). In an appealing hypothetical scenario, blocking both oncolytic and immunological pathways with an impact on *PD-L1* mRNA expression could improve immunotherapy efficiency on top of the effect achieved from PD-L1 antibody-mediated blocking. The hereby-described findings show that attempts to block type I and type II IFN signaling-mediated *PD-L1* expression at the mRNA level should in addition also consider the impact of type III IFN signaling.

5. Conclusion

This study describes that IFN-λ has the potential to induce PD-L1 and PD-L2 expression at least for some NSCLC cells. Given that *IFNL* mRNA and IFN-λ receptors can be co-expressed with *PD-L1* and *PD-L2* in NSCLC cell lines and tumors, the foundation for further study of IFN-λ-mediated regulation of PD-1-ligands *in vivo* and the consequence for achieving improved PD-1/PD-1-ligand immunotherapy is set.

CRediT authorship contribution statement

Trine Vilsbøll Larsen: Conceptualization, Data curation, Formal analysis, Methodology, Software, Validation, Visualization, Writing - original draft, Writing - review & editing.**Tina Fuglsang Daugaard:** Formal analysis, Validation, Writing - review & editing. **Hans Henrik Gad:** Conceptualization, Resources, Methodology, Writing - review & editing. **Rune Hartmann:** Conceptualization, Resources, Methodology, Writing - review & editing. **Anders Lade Nielsen:** Conceptualization, Data curation, Methodology, Software, Supervision, Visualization, Writing - review & editing.

Declaration of Competing Interest

The authors declare that they have no known competing financial interests or personal relationships that could have appeared to influence the work reported in this paper.

Data availability

Data will be made available on request.

Acknowledgments

Flow cytometry was performed at the FACS Core Facility, Aarhus University, Denmark. We thank the facility for the excellent help and guidance regarding the applied procedure. This study was supported by Direktør Emil C. Hertz og hustru Inger Hertz' Fond, StiboFonden, Knud og Edith Eriksens Mindefond, Inge og Jørgen Larsens Mindelegat, and Kræftfonden.

References

Ayers, M., Lunceford, J., Nebozhyn, M., Murphy, E., Loboda, A., Kaufman, D.R., Albright, A., Cheng, J.D., Kang, S.P., Shankaran, V., Piha-Paul, S.A., Yearley, J., Seiwert, T.Y., Ribas, A., McClanahan, T.K., 2017. IFN-gamma-related mRNA profile predicts clinical response to PD-1 blockade. J. Clin. Invest. 127 (8), 2930–2940.

Borghaei, H., Paz-Ares, L., Horn, L., Spigel, D.R., Steins, M., Ready, N.E., Chow, L.Q., Vokes, E.E., Felip, E., Holgado, E., Barlesi, F., Kohlhaufl, M., Arrieta, O., Burgio, M. A., Fayette, J., Lena, H., Poddubskaya, E., Gerber, D.E., Gettinger, S.N., Rudin, C.M., Rizvi, N., Crino, L., Blumenschein Jr., G.R., Antonia, S.J., Dorange, C., Harbison, C. T., Graf Finckenstein, F., Brahmer, J.R., 2015. Nivolumab versus docetaxel in advanced nonsquamous non-small-cell lung cancer. N. Engl. J. Med. 373 (17), 1627–1639.

Brand, S., Beigel, F., Olszak, T., Zitzmann, K., Eichhorst, S.T., Otte, J.M., Diebold, J., Diepolder, H., Adler, B., Auernhammer, C.J., Goke, B., Dambacher, J., 2005. IL-28A and IL-29 mediate antiproliferative and antiviral signals in intestinal epithelial cells and murine CMV infection increases colonic IL-28A expression. Am. J. Physiol. Gastrointest. Liver Physiol. 289 (5), G960–G968.

Burr, M.L., Sparbier, C.E., Chan, Y.C., Williamson, J.C., Woods, K., Beavis, P.A., Lam, E.Y. N., Henderson, M.A., Bell, C.C., Stolzenburg, S., Gilan, O., Bloor, S., Noori, T., Morgens, D.W., Bassik, M.C., Neeson, P.J., Behren, A., Darcy, P.K., Dawson, S.J., Voskoboinik, I., Trapani, J.A., Cebon, J., Lehner, P.J., Dawson, M.A., 2017. CMTM6 maintains the expression of PD-L1 and regulates anti-tumour immunity. Nature 549 (7670), 101–105.

Cerami, E., Gao, J., Dogrusoz, U., Gross, B.E., Sumer, S.O., Aksoy, B.A., Jacobsen, A., Byrne, C.J., Heuer, M.L., Larsson, E., Antipin, Y., Reva, B., Goldberg, A.P., Sander, C., Schultz, N., 2012. The cBio cancer genomics portal: an open platform for exploring multidimensional cancer genomics data. Cancer Discov. 2 (5), 401–404.

Chen, J., Markelc, B., Kaeppler, J., Ogundipe, V.M.L., Cao, Y., McKenna, W.G., Muschel, R.J., 2018. STING-dependent interferon-lambda1 induction in HT29 cells, a human colorectal cancer cell line, after gamma-radiation. Int. J. Radiat. Oncol. Biol. Phys. 101 (1), 97–106.

Chen, J., Yang, H., Teo, A.S.M., Amer, L.B., Sherbaf, F.G., Tan, C.Q., Alvarez, J.J.S., Lu, B., Lim, J.Q., Takano, A., Nahar, R., Lee, Y.Y., Phua, C.Z.J., Chua, K.P., Suteja, L., Chen, P.J., Chang, M.M., Koh, T.P.T., Ong, B.H., Anantham, D., Hsu, A.A.L., Gogna, A., Too, C.W., Aung, Z.W., Lee, Y.F., Wang, L., Lim, T.K.H., Wilm, A., Choi, P. S., Ng, P.Y., Toh, C.K., Lim, W.T., Ma, S., Lim, B., Liu, J., Tam, W.L., Skanderup, A.J., Yeong, J.P.S., Tan, E.H., Creasy, C.L., Tan, D.S.W., Hillmer, A.M., Zhai, W., 2020. Genomic landscape of lung adenocarcinoma in East Asians. Nat. Genet. 52 (2), 177–186.

Crotta, S., Davidson, S., Mahlakoiv, T., Desmet, C.J., Buckwalter, M.R., Albert, M.L., Staeheli, P., Wack, A., 2013. Type I and type III interferons drive redundant amplification loops to induce a transcriptional signature in influenza-infected airway epithelia. PLoS Pathog. 9 (11), e1003773.

Deb, P., Dai, J., Singh, S., Kalyoussef, E., Fitzgerald-Bocarsly, P., 2020. Triggering of the cGAS-STING pathway in human plasmacytoid dendritic cells inhibits TLR9-mediated IFN production. J. Immunol. 205 (1), 223–236.

Dellgren, C., Gad, H.H., Hamming, O.J., Melchjorsen, J., Hartmann, R., 2009. Human interferon-lambda 3 is a potent member of the type III interferon family. Genes Immun. 10 (2), 125–131.

Der, S.D., Zhou, A., Williams, B.R., Silverman, R.H., 1998. Identification of genes differentially regulated by interferon alpha, beta, or gamma using oligonucleotide arrays. PNAS 95 (26), 15623–15628.

Donnelly, R.P., Sheikh, F., Kotenko, S.V., Dickensheets, H., 2004. The expanded family of class II cytokines that share the IL-10 receptor-2 (IL-10R2) chain. J. Leukoc. Biol. 76 (2), 314–321.

Doyle, S.E., Schreckhise, H., Khuu-Duong, K., Henderson, K., Rosler, R., Storey, H., Yao, L., Liu, H., Barahmand-pour, F., Sivakumar, P., Chan, C., Birks, C., Foster, D., Clegg, C.H., Wietzke-Braun, P., Mihm, S., Klucher, K.M., 2006. Interleukin-29 uses a type 1 interferon-like program to promote antiviral responses in human hepatocytes. Hepatology 44 (4), 896–906.

Fehrenbacher, L., Spira, A., Ballinger, M., Kowanetz, M., Vansteenkiste, J., Mazieres, J., Park, K., Smith, D., Artal-Cortes, A., Lewanski, C., Braiteh, F., Waterkamp, D., He, P., Zou, W., Chen, D.S., Yi, J., Sandler, A., Rittmeyer, A., Group, P.S., 2016. Atezolizumab versus docetaxel for patients with previously treated non-small-cell

lung cancer (POPLAR): a multicentre, open-label, phase 2 randomised controlled trial. Lancet 387 (10030), 1837–1846.
Fujie, H., Tanaka, T., Tagawa, M., Kaijun, N., Watanabe, M., Suzuki, T., Nakayama, K., Numasaki, M., 2011. Antitumor activity of type III interferon alone or in combination with type I interferon against human non-small cell lung cancer. Cancer Sci. 102 (11), 1977–1990.
Gao, J., Aksoy, B.A., Dogrusoz, U., Dresdner, G., Gross, B., Sumer, S.O., Sun, Y., Jacobsen, A., Sinha, R., Larsson, E., Cerami, E., Sander, C., Schultz, N., 2013. Integrative analysis of complex cancer genomics and clinical profiles using the cBioPortal. Sci. Signal. 6 (269), pl1.
Gao, Y., Yang, J., Cai, Y., Fu, S., Zhang, N., Fu, X., Li, L., 2018. IFN-gamma-mediated inhibition of lung cancer correlates with PD-L1 expression and is regulated by PI3K-AKT signaling. Int. J. Cancer 143 (4), 931–943.
Garcia-Diaz, A., Shin, D.S., Moreno, B.H., Saco, J., Escuin-Ordinas, H., Rodriguez, G.A., Zaretsky, J.M., Sun, L., Hugo, W., Wang, X., Parisi, G., Saus, C.P., Torrejon, D.Y., Graeber, T.G., Comin-Anduix, B., Hu-Lieskovan, S., Damoiseaux, R., Lo, R.S., Ribas, A., 2019. Interferon receptor signaling pathways regulating PD-L1 and PD-L2 expression. Cell Rep. 29 (11), 3766.
Garon, E.B., Rizvi, N.A., Hui, R., Leighl, N., Balmanoukian, A.S., Eder, J.P., Patnaik, A., Aggarwal, C., Gubens, M., Horn, L., Carcereny, E., Ahn, M.J., Felip, E., Lee, J.S., Hellmann, M.D., Hamid, O., Goldman, J.W., Soria, J.C., Dolled-Filhart, M., Rutledge, R.Z., Zhang, J., Lunceford, J.K., Rangwala, R., Lubiniecki, G.M., Roach, C., Emancipator, K., Gandhi, L., Investigators, K., 2015. Pembrolizumab for the treatment of non-small-cell lung cancer. N. Engl. J. Med. 372 (21), 2018–2028.
Gong, K., Guo, G., Panchani, N., Bender, M.E., Gerber, D.E., Minna, J.D., Fattah, F., Gao, B., Peyton, M., Kernstine, K., Mukherjee, B., Burma, S., Chiang, C.M., Zhang, S., Amod Sathe, A., Xing, C., Dao, K.H., Zhao, D., Akbay, E.A., Habib, A.A., 2020. EGFR inhibition triggers an adaptive response by co-opting antiviral signaling pathways in lung cancer. Nat. Cancer 1 (4), 394–409.
Haragan, A., Field, J.K., Davies, M.P.A., Escriu, C., Gruver, A., Gosney, J.R., 2019. Heterogeneity of PD-L1 expression in non-small cell lung cancer: Implications for specimen sampling in predicting treatment response. Lung Cancer 134, 79–84.
He, J., Hu, Y., Hu, M., Li, B., 2015. Development of PD-1/PD-L1 pathway in tumor immune microenvironment and treatment for non-small cell lung cancer. Sci. Rep. 5, 13110.
Hirano, F., Kaneko, K., Tamura, H., Dong, H., Wang, S., Ichikawa, M., Rietz, C., Flies, D. B., Lau, J.S., Zhu, G., Tamada, K., Chen, L., 2005. Blockade of B7–H1 and PD-1 by monoclonal antibodies potentiates cancer therapeutic immunity. Cancer Res. 65 (3), 1089–1096.
Hu, X., Lin, Z., Wang, Z., Zhou, Q., 2021. Emerging role of PD-L1 modification in cancer immunotherapy. Am. J. Cancer Res. 11 (8), 3832–3840.
Hubert, M., Gobbini, E., Couillault, C., Manh, T.V., Doffin, A.C., Berthet, J., Rodriguez, C., Ollion, V., Kielbassa, J., Sajous, C., Treilleux, I., Tredan, O., Dubois, B., Dalod, M., Bendriss-Vermare, N., Caux, C., Valladeau-Guilemond, J., 2020. IFN-III is selectively produced by cDC1 and predicts good clinical outcome in breast cancer. Sci. Immunol. 5 (46).
Hwang, S., Kwon, A.Y., Jeong, J.Y., Kim, S., Kang, H., Park, J., Kim, J.H., Han, O.J., Lim, S.M., An, H.J., 2020. Immune gene signatures for predicting durable clinical benefit of anti-PD-1 immunotherapy in patients with non-small cell lung cancer. Sci. Rep. 10 (1), 643.
Iwai, Y., Ishida, M., Tanaka, Y., Okazaki, T., Honjo, T., Minato, N., 2002. Involvement of PD-L1 on tumor cells in the escape from host immune system and tumor immunotherapy by PD-L1 blockade. PNAS 99 (19), 12293–12297.
Jenkins, R.W., Barbie, D.A., Flaherty, K.T., 2018. Mechanisms of resistance to immune checkpoint inhibitors. Br. J. Cancer 118 (1), 9–16.
Kotenko, S.V., Gallagher, G., Baurin, V.V., Lewis-Antes, A., Shen, M., Shah, N.K., Langer, J.A., Sheikh, F., Dickensheets, H., Donnelly, R.P., 2003. IFN-lambdas mediate antiviral protection through a distinct class II cytokine receptor complex. Nat. Immunol. 4 (1), 69–77.
Lai, Q., Wang, H., Li, A., Xu, Y., Tang, L., Chen, Q., Zhang, C., Gao, Y., Song, J., Du, Z., 2018. Decitibine improve the efficiency of anti-PD-1 therapy via activating the response to IFN/PD-L1 signal of lung cancer cells. Oncogene 37 (17), 2302–2312.
Larsen, T.V., Hussmann, D., Nielsen, A.L., 2019. PD-L1 and PD-L2 expression correlated genes in non-small-cell lung cancer. Cancer Commun. (Lond.) 39 (1), 30.
Larsen, T.V., Dybdal, N., Daugaard, T.F., Lade-Keller, J., Lin, L., Sorensen, B.S., Nielsen, A.L., 2023. Examination of the functional relationship between PD-L1 DNA methylation and mRNA expression in non-small-cell lung cancer. Cancers 15 (6).
Lasfar, A., Zloza, A., Silk, A.W., Lee, L.Y., Cohen-Solal, K.A., 2019. Interferon lambda: toward a dual role in cancer. J. Interferon Cytokine Res. 39 (1), 22–29.
Lauber, C., Vieyres, G., Terczynska-Dyla, E., Anggakusuma, R., Dijkman, H.H., Gad, H., Akhtar, R., Geffers, F.W., Vondran, V., Thiel, L., Kaderali, T., Pietschmann, R.H., 2015. Transcriptome analysis reveals a classical interferon signature induced by IFNlambda4 in human primary cells. Genes Immun. 16 (6), 414–421.
Lee, S.J., Jang, B.C., Lee, S.W., Yang, Y.I., Suh, S.I., Park, Y.M., Oh, S., Shin, J.G., Yao, S., Chen, L., Choi, I.H., 2006. Interferon regulatory factor-1 is prerequisite to the constitutive expression and IFN-gamma-induced upregulation of B7–H1 (CD274). FEBS Lett. 580 (3), 755–762.
Li, W., Huang, X., Liu, Z., Wang, Y., Zhang, H., Tong, H., Wu, H., Lin, S., 2012. Type III interferon induces apoptosis in human lung cancer cells. Oncol. Rep. 28 (3), 1117–1125.
Lu, R., Au, W.C., Yeow, W.S., Hageman, N., Pitha, P.M., 2000. Regulation of the promoter activity of interferon regulatory factor-7 gene. Activation by interferon snd silencing by hypermethylation. J. Biol. Chem. 275 (41), 31805–31812.
Malhotra, J., Jabbour, S.K., Aisner, J., 2017. Current state of immunotherapy for non-small cell lung cancer. Transl. Lung Cancer Res. 6 (2), 196–211.
Mehnert, J.M., Monjazeb, A.M., Beerthuijzen, J.M.T., Collyar, D., Rubinstein, L., Harris, L.N., 2017. The challenge for development of valuable immuno-oncology biomarkers. Clin. Cancer Res. 23 (17), 4970–4979.
Mezzadra, R., Sun, C., Jae, L.T., Gomez-Eerland, R., de Vries, E., Wu, W., Logtenberg, M. E.W., Slagter, M., Rozeman, E.A., Hofland, I., Broeks, A., Horlings, H.M., Wessels, L. F.A., Blank, C.U., Xiao, Y., Heck, A.J.R., Borst, J., Brummelkamp, T.R., Schumacher, T.N.M., 2017. Identification of CMTM6 and CMTM4 as PD-L1 protein regulators. Nature 549 (7670), 106–110.
Morimoto, Y., Kishida, T., Kotani, S.I., Takayama, K., Mazda, O., 2018. Interferon-beta signal may up-regulate PD-L1 expression through IRF9-dependent and independent pathways in lung cancer cells. Biochem. Biophys. Res. Commun. 507 (1–4), 330–336.
Platanias, L.C., 2005. Mechanisms of type-I- and type-II-interferon-mediated signalling. Nat. Rev. Immunol. 5 (5), 375–386.
Prokunina-Olsson, L., Muchmore, B., Tang, W., Pfeiffer, R.M., Park, H., Dickensheets, H., Hergott, D., Porter-Gill, P., Mumy, A., Kohaar, I., Chen, S., Brand, N., Tarway, M., Liu, L., Sheikh, F., Astemborski, J., Bonkovsky, H.L., Edlin, B.R., Howell, C.D., Morgan, T.R., Thomas, D.L., Rehermann, B., Donnelly, R.P., O'Brien, T.R., 2013. A variant upstream of IFNL3 (IL28B) creating a new interferon gene IFNL4 is associated with impaired clearance of hepatitis C virus. Nat. Genet. 45 (2), 164–171.
M. Reck, D. Rodriguez-Abreu, A.G. Robinson, R. Hui, T. Csoszi, A. Fulop, M. Gottfried, N. Peled, A. Tafreshi, S. Cuffe, M. O'Brien, S. Rao, K. Hotta, M.A. Leiby, G.M. Lubiniecki, Y. Shentu, R. Rangwala, J.R. Brahmer, K.-. Investigators, Pembrolizumab versus chemotherapy for PD-L1-positive non-small-cell lung cancer, N Engl J Med 375(19) (2016) 1823-1833.
Sheppard, P., Kindsvogel, W., Xu, W., Henderson, K., Schlutsmeyer, S., Whitmore, T.E., Kuestner, R., Garrigues, U., Birks, C., Roraback, J., Ostrander, C., Dong, D., Shin, J., Presnell, S., Fox, B., Haldeman, B., Cooper, E., Taft, D., Gilbert, T., Grant, F.J., Tackett, M., Krivan, W., McKnight, G., Clegg, C., Foster, D., Klucher, K.M., 2003. IL-28, IL-29 and their class II cytokine receptor IL-28R. Nat. Immunol. 4 (1), 63–68.
Shibahara, D., Tanaka, K., Iwama, E., Kubo, N., Ota, K., Azuma, K., Harada, T., Fujita, J., Nakanishi, Y., Okamoto, I., 2018. Intrinsic and extrinsic regulation of PD-L2 expression in oncogene-driven non-small cell lung cancer. J. Thorac. Oncol. 13 (7), 926–937.
Skafi, N., Fayyad-Kazan, M., Badran, B., 2020. Immunomodulatory role for MicroRNAs: regulation of PD-1/PD-L1 and CTLA-4 immune checkpoints expression. Gene 754, 144888.
Sommereyns, C., Paul, S., Staeheli, P., Michiels, T., 2008. IFN-lambda (IFN-lambda) is expressed in a tissue-dependent fashion and primarily acts on epithelial cells in vivo. PLoS Pathog. 4 (3), e1000017.
Sumimoto, H., Takano, A., Teramoto, K., Daigo, Y., 2016. RAS-mitogen-activated protein kinase signal is required for enhanced PD-L1 expression in human lung cancers. PLoS One 11 (11), e0166626.
Sun, J.Y., Zhang, D., Wu, S., Xu, M., Zhou, X., Lu, X.J., Ji, J., 2020. Resistance to PD-1/PD-L1 blockade cancer immunotherapy: mechanisms, predictive factors, and future perspectives. Biomark. Res. 8, 35.
Tezuka, Y., Endo, S., Matsui, A., Sato, A., Saito, K., Semba, K., Takahashi, M., Murakami, T., 2012. Potential anti-tumor effect of IFN-lambda2 (IL-28A) against human lung cancer cells. Lung Cancer 78 (3), 185–192.
Thomsen, R., Solvsten, C.A., Linnet, T.E., Blechingberg, J., Nielsen, A.L., 2010. Analysis of qPCR data by converting exponentially related Ct values into linearly related X0 values. J. Bioinform. Comput. Biol. 8 (5), 885–900.
Udall, M., Rizzo, M., Kenny, J., Doherty, J., Dahm, S., Robbins, P., Faulkner, E., 2018. PD-L1 diagnostic tests: a systematic literature review of scoring algorithms and test-validation metrics. Diagn. Pathol. 13 (1), 12.
Vitiello, G.A.F., Ferreira, W.A.S., Cordeiro de Lima, V.C., Medina, T.D.S., 2021. Antiviral responses in cancer: boosting antitumor immunity through activation of interferon pathway in the tumor microenvironment. Front. Immunol. 12, 782852.
Wack, A., Terczynska-Dyla, E., Hartmann, R., 2015. Guarding the frontiers: the biology of type III interferons. Nat. Immunol. 16 (8), 802–809.
Walter, M.R., 2020. The role of structure in the biology of interferon signaling. Front. Immunol. 11, 606489.
Zanoni, I., Granucci, F., Broggi, A., 2017. Interferon (IFN)-lambda takes the helm: immunomodulatory roles of type III IFNs. Front. Immunol. 8, 1661.
Zhou, Z., Hamming, O.J., Ank, N., Paludan, S.R., Nielsen, A.L., Hartmann, R., 2007. Type III interferon (IFN) induces a type I IFN-like response in a restricted subset of cells through signaling pathways involving both the Jak-STAT pathway and the mitogen-activated protein kinases. J. Virol. 81 (14), 7749–7758.